AN INFORMED NMF-BASED UNMIXING APPROACH FOR MINERAL DETECTION AND MAPPING IN THE ALGERIAN CENTRAL HOGGAR USING PRISMA REMOTE SENSING HYPERSPECTRAL DATA

Fatima Zohra Benhalouche [1, 2, 3], *Oussama Benabbou* [1], *Lahsen Wahib Kebir* [1], *Ahmed Bennia* [1], *Moussa Sofiane Karoui* [1, 2, 3] and *Yannick Deville* [2]

[1] Agence Spatiale Algérienne, Centre des Techniques Spatiales, Arzew, Algérie
[2] IRAP, Université de Toulouse, UPS-OMP, CNRS, CNES, Toulouse, France
[3] LSI, Université des Sciences et de la Technologie d'Oran Mohamed Boudiaf, Oran, Algérie

{Fatima.Benhalouche, Sofiane.Karoui, Yannick.Deville}@irap.omp.eu,
{obenabbou, wkebir, abennia}@cts.asal.dz

IGARSS 2021 - 2021 IEEE International Geoscience and Remote Sensing Symposium | 978-1-6654-0369-6/21/$31.00 ©2021 IEEE | DOI: 10.1109/IGARSS47720.2021.9553414

ABSTRACT

In these investigations, an informed unmixing-based approach is considered for detecting and mapping several mineral deposits in the Algerian Central Hoggar. The considered technique, which is related to linear spectral unmixing methods, uses an informed multiplicative nonnegative matrix factorization algorithm. This technique unmixes the used hyperspectral remote sensing data by exploiting known spectra of the considered minerals. Experiments are carried out, to assess the potential of the used technique, on real hyperspectral PRecursore IperSpettrale della Missione Applicativa (PRISMA) data, which cover the considered study area. Obtained maps are analyzed by using a geological map of the investigated region.

Index Terms— Mineral mapping, PRISMA remote sensing hyperspectral data, linear spectral unmixing, informed nonnegative matrix factorization.

1. INTRODUCTION

In recent years, remote sensing has been widely used for lithological mapping and mineral exploration. Different remote sensing data have been used, in particular for geological studies of very large or inaccessible areas, in order to save time in mining exploration [1]-[3].

During the last twenty years, the mostly remote sensing data for geological mapping and mineral exploration applications, include those from Landsat, Advanced Spaceborne Thermal Emission and Reflection (ASTER) or Sentinel-2 multispectral sensors [4]-[7]. However, due to the limitation of their spectral resolution, these multispectral data do not provide sufficient accuracy for precise mineralogical mapping.

Recently, hyperspectral sensors have gained attention due to their high spectral resolution. This spectral characteristic allows better identification and classification of surface mineralogy [8]-[10].

Thus, several methods, involving hyperspectral remote sensing data, are considered for detecting and mapping several minerals, such as approaches that use: spectral band ratios [11], Principal Components Analysis (PCA) [12], [13], and Spectral Angle Mapper (SAM) [14], [15]. Obtained results, from these approaches, are not very precise, due to the low spatial resolution of the considered hyperspectral remote sensing data. Indeed, due to this low spatial resolution, mixed pixels, composed of several endmembers, may be present in the considered data. Such a configuration prevents direct detection and area estimation, by using standard techniques, of these pure materials. For that reason, advanced processing methods, to unmix these mixed spectra, are necessary.

Linear spectral unmixing (LSU) approaches [16] are the main considered techniques for realizing the necessary unmixing procedure. These approaches linearly decompose observed pixel spectra into a collection of pure material spectra and a set of associated abundance fractions, which correspond to the proportion of each pure material present in each observed pixel [16].

Recently, a remote sensing LSU-based technique was used for detecting and mapping Kaolinite deposits in the Algerian Central Hoggar [17]. This technique, reported in [18], is based on informed (or partial) Nonnegative Matrix Factorization (NMF) [19], and was used to exploit known spectra of the Kaolinite, by means of multiplicative update rules, to unmix ASTER multispectral data, which cover the considered region, in order to obtain the abundance fraction map of the Kaolinite. It should be noted here that in that work, only one material (i.e. the Kaolinite) is considered to be known due to the use of multispectral data that do not allow a precise discrimination between several materials.

In the investigations reported here, the same partial NMF-unmixing-based technique is considered for detecting and mapping several mineral deposits, in the same area, by using PRecursore IperSpettrale della Missione Applicativa (PRISMA) [20] remote sensing hyperspectral data. These minerals are: Quartz, Muscovite, Muscovite-Pyrophyllite, Kaolinite, Alunite-Pyrophyllite, Alunite-Kaolinite, Hematite-Quartz, Goethite-Phyllite, and Chlorite-Muscovite. The used technique here also exploits known spectra of these minerals. Unlike the previous work [17], here the use of hyperspectral data allows a better differentiation between the above minerals, thus justifying their consideration in these investigations.

The remainder of this paper is organized as follows. The considered hyperspectral data and study area are described in Section 2. The used approach is briefly presented in Section 3. In Section 4, the conducted experiments are described. Finally, a conclusion is given in Section 5.

2. USED DATA AND STUDY AREA

As stated above, PRISMA remote sensing hyperspectral data are used in these investigations. PRISMA is a hyperspectral mission launched by the Italian Space Agency (ASI) on March 22, 2019. It uses a spaceborne hyperspectral sensor, which provides data with a spatial resolution of 30 m and 230 spectral bands in the 0.4-2.5 µm wavelength domain [20]. The high spectral resolution of this hyperspectral sensor allows discriminating and accurately classifying a variety of minerals and rock types, making it an efficient tool for mineral detecting and mapping.

The objective of this study is to evaluate the performance of the used method, applied to PRISMA hyperspectral data, for mineral detecting and mapping.

The manipulated image is geometrically and atmospherically corrected.

The study area, called “Issalane” (Fig. 1), is located in the Algerian Central Hoggar. This part of the Hoggar region concentrates the main mountain ranges that have crystalline and metamorphic origins.

It is characterized by its geological diversities and geomorphological units [21]. Geologically, this area presents a great interest due to its considerable mineral potential. Indeed, valuable gold and copper deposits, and base-metal mineralization have been located in that region.

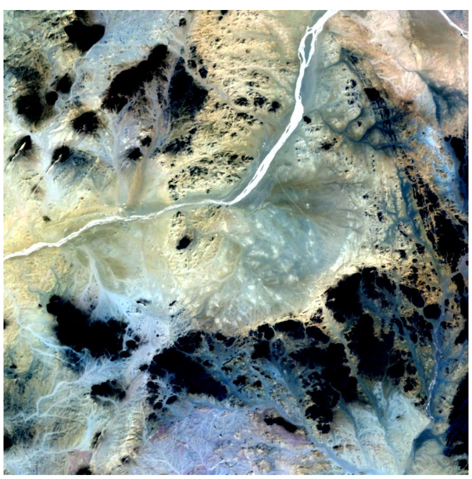

Figure 1. True color image composite, from PRISMA hyperspectral data, of the considered “Issalane” study area.

3. CONSIDERED APPROACH

As mentioned above, the technique reported in [17], [18] is used in this work. This informed linear NMF-based approach takes advantage of the nonnegativity property of a manipulated remote sensing hyperspectral image $X \in R_{+}^{N\times K}$ for its unmixing. N and K represent, respectively, the numbers of spectral bands and pixels of this image. This matrix is modeled as [17], [18]

$$X = (A_1 + A_2) S = A_1 S + A_2 S. \quad (1)$$

The columns of the two matrices A_1 and $A_2 \in R_{+}^{N\mathrm{x}L}$ contain, respectively, known and unknown pure material spectra. The number of all these pure materials is represented by L, which may be estimated by the Hyperspectral Signal subspace identification by minimum error (HySime) [22] technique. The first L_1 columns of the first matrix A_1 are related to the known mineral spectra. The other columns of this first matrix are composed of zeros. The last L_2 columns of the second matrix A_2 are related to the unknown pure material spectra. The other columns of this second matrix are composed of zeros. Obviously, $L = L_1 + L_2$.

The matrix $S \in R_{+}^{L\mathrm{x}K}$ contains, in each of its rows, all nonnegative abundance fractions, in all pixels, of one, known or unknown, pure material. Evidently, the sum of these abundance fractions is equal to one in each pixel of the considered image [17].

In (1), the unknown matrices that will be estimated by the used method are A_2 and, especially, the abundance fractions in S of the considered minerals. These abundance fractions allow the detection and mapping of these minerals.

The considered method optimizes the following criterion

$$J = \frac{1}{2} \left\| X - A_1 \tilde{S} - \tilde{A}_2 \tilde{S} \right\|_{\mathrm{F}}^2, \quad (2)$$

where $\tilde{A}_2$ and $\tilde{S}$ aim at estimating, respectively, A_2 and S. $\|.\|_{\mathrm{F}}$ denotes the Frobenius norm.

The minimization process is achieved, after the initialization step performed as mentioned in [17], by means of the following iterative and multiplicative update rules

$$\tilde{A}_2 \leftarrow \tilde{A}_2 \odot X\tilde{S}^{\mathrm{T}} \oslash (A_1\tilde{S}\tilde{S}^{\mathrm{T}} + \tilde{A}_2\tilde{S}\tilde{S}^{\mathrm{T}} + \varepsilon), \quad (3)$$

$$\tilde{S} \leftarrow \tilde{S} \odot (A_1^{\mathrm{T}}X + \tilde{A}_2^{\mathrm{T}}X) \oslash (\tilde{A}_2^{\mathrm{T}}A_1\tilde{S} + A_1^{\mathrm{T}}\tilde{A}_2\tilde{S} + A_1^{\mathrm{T}}A_1\tilde{S} + \tilde{A}_2^{\mathrm{T}}\tilde{A}_2\tilde{S} + \varepsilon). \quad (4)$$

The operator $\odot$ (respectively $\oslash$) corresponds to the element-wise multiplication (respectively division). $(.)^{\mathrm{T}}$ denotes the matrix transpose, and ε (a very small and positive value) allows avoiding divisions by zero.

4. OBTAINED RESULTS

As introduced, experiments are conducted by using PRISMA remote sensing hyperspectral data that cover the considered study area.

In the conducted experiments, the number L of all (known and unknown) pure materials is estimated, by the HySime technique, at 15. Again, and mentioned above, nine spectra, of the considered minerals (i.e. Quartz, Muscovite,

Muscovite-Pyrophyllite, Kaolinite, Alunite-Pyrophyllite, Alunite-Kaolinite, Hematite-Quartz, Goethite-Phyllite, and Chlorite-Muscovite) that are present in the studied area, are used, as known spectra (i.e., L_1=9, and therefore, L_2=6). The original spectra of these minerals are obtained from the U.S. Geological Survey (USGS) spectral library [23]. These spectra are resampled (Fig. 2) to match the spectral bands considered in the processed PRISMA image.

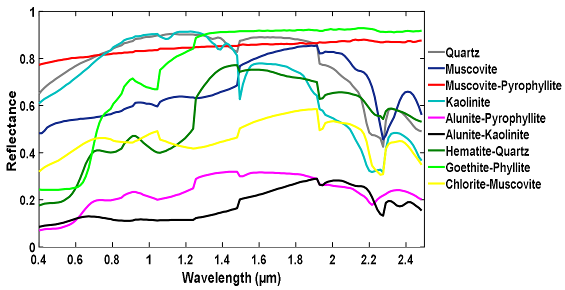

Figure 2. The resampled known mineral spectra.

After execution of the considered algorithm on the above PRISMA hyperspectral image, by considering the above nine resampled known mineral spectra and also the six unknown pure material spectra, the obtained abundance fraction maps of these pure materials are given in the next figure (Fig. 3(a)-(j)). These obtained maps are analyzed and compared by using a geological map (Fig. 3(k)) of the investigated region.

(a) Quartz

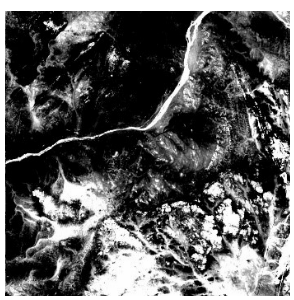

(b) Muscovite

(c) Muscovite-Pyrophyllite

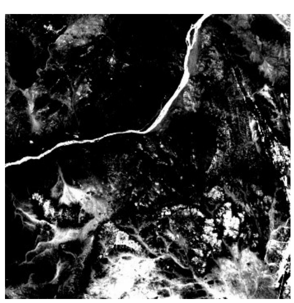

(d) Kaolinite

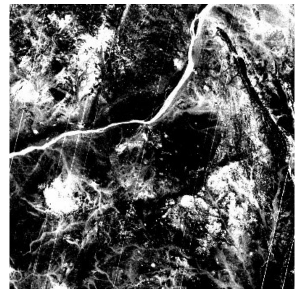

(e) Alunite-Pyrophyllite

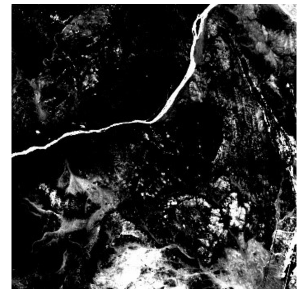

(f) Alunite-Kaolinite

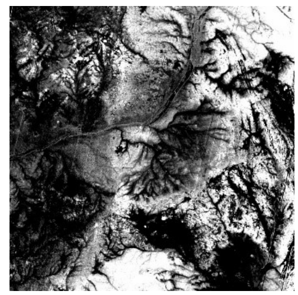

(g) Hematite-Quartz

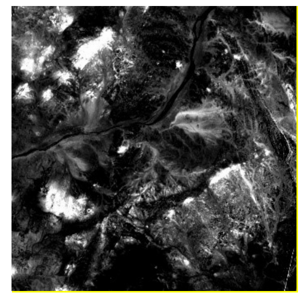

(h) Goethite-Phyllite

(i) Chlorite-Muscovite

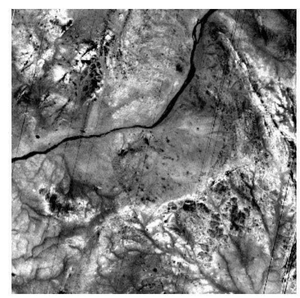

(j)

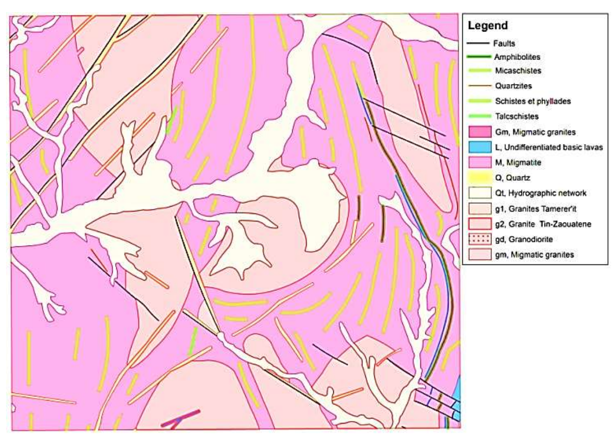

(k)

Figure 3. (a)-(i) Obtained abundance fraction maps of the considered minerals. (j) The obtained map of the sum of the six unknown pure material abundance fractions.
(k) A geological map of the considered study area.

Globally, the above figure shows a good correlation between the obtained abundance fraction maps of the nine considered minerals and the geological units included in the used geological map, in terms of lithology and mineral groups. Also, this figure confirms that the used approach, applied to the considered PRISMA hyperspectral image, is very attractive for detecting and mapping these minerals in the considered study area.

5. CONCLUSION

In this work, the potential of an informed linear NMF-unmixing-based approach, applied to PRISMA remote sensing hyperspectral data for detecting and mapping nine minerals in the Algerian Central Hoggar region, is investigated.

The considered approach uses a nonnegative matrix factorization algorithm that takes advantage of the nonnegativity property of manipulated data and also exploits the known spectra of minerals to be detected and mapped.

The obtained abundance fraction maps of the considered minerals were analyzed and compared by using a geological map of the investigated area. Globally, there is a good correlation between the obtained abundance fraction maps of the nine considered minerals and the geological units included in the used geological map, in terms of lithology and mineral groups.

6. REFERENCES

[1] A. Goetz, F. Billingsley, D. Elston, I. Lucchitta, E. Shoemaker, M. Abrams, A. Gillespie, R. Squires, "Applications of ERTS Images and Image Processing to Regional Problems and Geologic Mapping in Northern Arizona," *NASA/JPL Technical Reports*, 32-1597, NASA, Pasadena, CA, USA, 1975.

[2] R. Baker, "Landsat Data: A new perspective for geology," *Photogrammetric Engineering and Remote Sensing*, 41(10), pp. 1233–1239, 1975.

[3] B. S. Siegal, A. R. Gillespie, *Remote Sensing in Geology*, Wiley, New York, NY, USA, 1980.

[4] T. Cudahy and R. Hewson, "ASTER geological case histories: Porphyry-skarn-epithermal, iron oxide Cu-Au and Broken Hill Pb-Zn-Ag," *In Proc. of the Annual General Meeting of the Geological Remote Sensing Group* (ASTER Unveiled), London, UK, 2002.

[5] F. D. van der Meer, H. van der Werff, and F. van Ruitenbeek, "Potential of ESA's Sentinel-2 for geological applications," *Remote Sensing and Environment*, 148, pp. 124–133, 2014.

[6] W. Ge, Q. Cheng, L. Jing, C. Armenakis, and H. Ding, "Lithological discrimination using ASTER and Sentinel-2A in the Shibanjing ophiolite complex of Beishan orogenic in Inner Mongolia, China," *Advances in Space Research*, 62(7), pp. 1702–1716, 2018.

[7] M. Abrams and Y. Yamaguchi, "Twenty Years of ASTER Contributions to Lithologic Mapping and Mineral Exploration," *Remote Sensing*, 11(11), 1394, 2019.

[8] S. Chabrillat, P. Pinet, G. Ceuleneer, P. Johnson and J. Mustrad, "Ronda Peridotite Massif: Methodology for its Geological Mapping and Lithological Discrimination from Airborne Hyperspectral Data," *International Journal of Remote Sensing*, 21(12), pp. 2363–2388, 2000.

[9] S. Chevrel, V. Kuosmannen, R. Belocky, S. Marsh, T. Tapani, H. Mollat, L. Quental, P. Vosen, V. Schumacher, E. Kuronen and P. Aastrup, "Hyperspectral Airborne Imagery for Mapping Mining-Related Contaminated Areas in Various European Environments - First Results of the MINEO Project," *5th International Airborne Remote Sensing Conference*, 2001.

[10] T. Cudahy, R. Hewson, J. Huntington, M. Quigley and P.S. Barry, "The Performance of the Satellite-Borne HYPERION Hyperspectral VNIR-SWIR Imaging System for Mineral Mapping at Mount Fitton, South Australia," *In Proc. IEEE International Geoscience and Remote Sensing Symposium* (IEEE IGARSS 2001), Sydney, NSW, Australia, 2001.

[11] F.J.A. Van Ruitenbeek, P. Debba, F.D. Van der Meer, T. Cudahy, M. Van der Meijde, M. Hale, "Mapping white micas and their absorption wavelengths using hyperspectral band ratios," *Remote Sensing and Environment*, 102, pp. 211–222, 2002.

[12] B. Yousefi, S. Sojasi, C. Ibarra Castanedo, G. Beaudoin, F. Huot, X. P. V. Maldague, M. Chamberland, and E. Lalonde, "Mineral identification in hyperspectral imaging using Sparse-PCA," *In Proc. of SPIE Commercial + Scientific Sensing and Imaging*, 9861, 2016.

[13] A. L. Machidon, F. Del Frate, M. Picchiani, O. M. Machidon and P. L. Ogrutan, "Geometrical Approximated Principal Component Analysis for Hyperspectral Image Analysis," *Remote Sensing*, 12(11), 2020.

[14] E. Hubbard, J. K. Crowley and D. R. Zimbelman, "Comparative alteration mineral mapping using visible to shortwave infrared (0.4–2.4 mm) Hyperion, ALI, and ASTER imagery". *IEEE Transactions on Geoscience and Remote Sensing*, 41, pp. 1401–1410, 2003.

[15] E. Hubbard and J. K. Crowley, "Mineral mapping on the Chilean–Bolivian Altiplano using co–orbital ALI, ASTER and Hyperion imagery: data dimensionality issues and solutions," *Remote Sensing and Environment*, 99, pp. 173–186, 2005.

[16] J. M. Bioucas-Dias, A. Plaza, N. Dobigeon, M. Parente, Q. Du, P. Gader, and J. Chanussot, "Hyperspectral Unmixing Overview: Geometrical, Statistical, and Sparse Regression-Based Approaches," *IEEE Journal of Selected Topics in Applied Earth Observations and Remote Sensing*, 5(2), pp. 354–379, 2012.

[17] F. Z. Benhalouche, O. Benabbou, M. S. Karoui, L. W. Kebir and Y. Deville, "Detecting and Mapping Kaolinite in the Algerian Central Hoggar with a Partial Linear NMF-Based Unmixing Method," *IEEE Mediterranean and Middle-East Geoscience and Remote Sensing Symposium* (IEEE M2GARSS 2020), Tunis, Tunisia, 2020.

[18] M.S. Karoui, F.Z. Benhalouche, Y. Deville, K. Djerriri, X. Briottet, T. Houet, A. Le Bris, and C. Weber, "Partial Linear NMF-Based Unmixing Methods for Detection and Area Estimation of Photovoltaic Panels in Urban Hyperspectral Remote Sensing Data," *Remote Sensing*, 11(18), pp. 2164, 2019.

[19] A. Cichocki, R. Zdunek, A.H. Phan, and S.-I. Amari, *Nonnegative matrix and tensor factorizations. Applications to exploratory multi-way data analysis and blind source separation*, Wiley, Chichester, UK, 2009.

[20] R. Loizzo, R. Guarini, F. Longo, T. Scopa, R. Formaro, C. Facchinetti and G. Varacalli "PRISMA: The Italian hyperspectral mission," *In Proc. IEEE International Geoscience and Remote Sensing Symposium* (IEEE IGARSS 2018), pp. 175–178, Valencia, Spain, 2018.

[21] J.M.L. Bertrand and R. Caby, "Geodynamic evolution of the Pan-African orogenic belt: a new interpretation of the Hoggar Shield (Algerian Sahara)," *Geologische Rundschau*, 67(2), pp. 357–388, 1978.

[22] J. M. Bioucas-Dias, J. M. P. Nascimento, "Hyperspectral subspace identification," *IEEE Transactions on Geoscience and Remote Sensing*, 46(8), pp. 2435-2445, 2008.

[23] R.N. Clark, G.A. Swayze, R. Wise, E. Livo, T. Hoefen, R. Kokaly, and S.J. Sutley, "USGS digital spectral library splib06a, U. S. Geological Survey," Digital Data Series, 231, (2007). http://speclab.cr.usgs.gov/spectral.lib06/